Solar Energy Materials and Solar Cells 186 (2018) 373–377

Contents lists available at ScienceDirect

Solar Energy Materials and Solar Cells

journal homepage: www.elsevier.com/locate/solmat

Impact of copper on light-induced degradation in Czochralski silicon PERC solar cells

C. Modanese[a], Mt. Wagner[b], F. Wolny[b], A. Oehlke[b], H.S. Laine[a], A. Inglese[a], H. Vahlman[a], M. Yli-Koski[a], H. Savin[a,*]

[a] Aalto University, Department of Electronics and Nanoengineering, Tietotie 3, 02150 Espoo, Finland
[b] SolarWorld Industries GmbH, Martin-Luther-King-Str. 24, 53175 Bonn, Germany

ARTICLE INFO

Keywords:
Copper
Light-induced degradation
PERC
Czochralski silicon
Cell efficiency
LID imaging

ABSTRACT

Both multicrystalline and Czochralski (Cz) silicon substrates are known to suffer from various mechanisms of light-induced degradation (LID), including copper-related LID (Cu-LID). Past studies on Cu-LID have mostly been performed on unprocessed wafers, omitting the impact of the solar cell process on the copper distribution. Here, we carefully contaminate Cz-substrates of different quality with different amounts of copper and process the substrates into complete industrial Cz-Si PERC solar cells, reaching a comprehensive mapping of the impact of Cu-LID for the PV industry. The results show that both the copper contamination level and Cz crystal quality are critical factors affecting the extent of Cu-LID. Most importantly, we show that copper can result in significant concentrations in the bulk of the finished PERC cells after being exposed to only trace surface contamination. Consequently, even a small local copper contamination area (~ 3–4 cm^2) is sufficient to induce strong LID in the full-sized (156 × 156 mm^2) cell parameters, resulting *e.g.* in ~7% relative efficiency loss during light soaking. The corresponding short circuit current density decreases by up to a factor of two in the contaminated areas.

1. Introduction

The silicon photovoltaics (PV) industry is now rapidly moving toward the passivated emitter and rear cell (PERC) architecture, which is expected to represent more than 55% of the global PV market by 2027 [1] and at present is already the industrial standard for high-efficiency solar cells. PERC cells are known to be highly sensitive for the bulk minority carrier lifetime, which explains the recent shift from multicrystalline silicon (mc-Si) to Czochralski silicon (Cz-Si) as the preferred substrate material. For the same reason, PERC cells are expected to suffer from various light-induced degradation (LID) mechanisms more than *e.g.* traditional aluminium back surface field (Al-BSF) cells. Degradation in PERC cells has indeed been shown for light and elevated temperature induced degradation (LeTID) [2,3] and boron-oxygen LID (BO-LID) [4–6], but it has not yet been shown for copper-related LID (Cu-LID) on Cz-Si substrates.

The impact of Cu-LID in crystalline silicon has been largely studied [7] and there is currently a good understanding of the physical mechanisms leading to Cu-LID [8,9]. Nevertheless, the vast majority of the data on this phenomenon has been obtained at wafer level (*i.e.* on lifetime or semi-fabricate samples). The feedstock is indeed one of the sources for copper contamination [9,10], although other sources appearing at later phases of the solar cell fabrication, such as brass wire wafer sawing [11], may be even more detrimental. Furthermore, given the extremely high solid diffusivity of copper in silicon even at low temperatures [12], Cu impurities tend to be ubiquitous and the high-temperature steps involved in PERC cell processing (*i.e.* phosphorus-emitter diffusion and metal contact firing) are particularly critical for their potential to drive-in Cu and contaminate the complete cell. At present, only very limited information on the impact of Cu-LID is available on fully-processed solar cells, namely only in PERC cells fabricated with quasi-monocrystalline silicon substrates [13] and in Al-BSF cells fabricated with mc-Si substrates [14]. Therefore, it is important to study the impact of Cu-LID in complete Cz-Si PERC devices.

In addition, silicon crystals with different qualities are processed within the PV industry, and it has been shown that the oxygen concentration in the silicon wafer bulk impacts the extent of the BO-LID, both at a wafer level [15] and on complete PERC solar cells fabricated with an industrial process [16]. While the impact of Cz crystal quality on the extent of Cu-LID has been reported at a wafer level [17], it still remains unknown at a solar cell level.

In this work, we perform a controlled Cu contamination experiment

* Corresponding author.
E-mail addresses: chiara.modanese@aalto.fi (C. Modanese), hele.savin@aalto.fi (H. Savin).

https://doi.org/10.1016/j.solmat.2018.07.006
Received 20 March 2018; Received in revised form 4 July 2018; Accepted 6 July 2018
Available online 18 July 2018
0927-0248/

on different Cz-Si materials with Cu concentrations relevant for industrial processes. We process the substrates into full-sized p-type PERC cells in an industrial manufacturing line and quantify the potential effect of Cu impurities on the LID they induce for the final cell parameters. The impact of the crystal quality on the retained LID is also evaluated.

2. Experimental

We used commercial pseudo-square 156 × 156 mm^2 B-doped Cz silicon sister wafers from two different ingots that were divided into two groups, accordingly. The ingots had a slightly different initial oxygen concentration and different thermal history resulting in different bulk micro defect (BMD) densities. In order to determine the BMD density, parallel as-cut wafers from both ingots were first polish etched and then Secco etched using standard recipes. The BMD density was then measured by etch pit density measurements, according to which the ingot groups are hereinafter defined, *i.e.* the high-BMD group has a BMD in the order of 4×10^5 cm^{-2}, whereas the low-BMD group features BMD concentrations below the detection limit ($\sim 10^3$ cm^{-2}). The wafers had resistivity of 1.8–2.0 Ωcm (high-BMD) and 1.8–2.2 Ωcm (low-BMD), thickness of ~ 190 μm, interstitial oxygen concentration, O_i of 8.5–9.5·10^{17} cm^{-3} (high-BMD) and 7–9 × 10^{17} cm^{-3} (low-BMD). The O_i concentration was measured by Fourier transform infrared spectroscopy (FTIR) on sister wafers, following the methodology described in Ref. [18].

The overall process flow chart is sketched in Fig. 1. The wafers were first cleaned in an industrial line, with an alkaline saw damage removal (SDR) followed by an acidic cleaning (*i.e.* in HCl and HF/O_3 solutions), and then packed in a dark box and delivered to the lab-scale cleanroom facilities for the Cu spot contamination. There, the intentional Cu contamination followed the same procedure as described in Ref. [19]. In order to obtain a controlled diffusion into the silicon bulk, the wafers were first cleaned with the standard RCA process, which was followed by double-sided thermal silicon dioxide growth (dry oxidation at 900 °C for 40 min in O_2, followed by a 20 min iso-temperature anneal in N_2). After thermal oxidation, three droplets (~ 20 mm diameter) with a

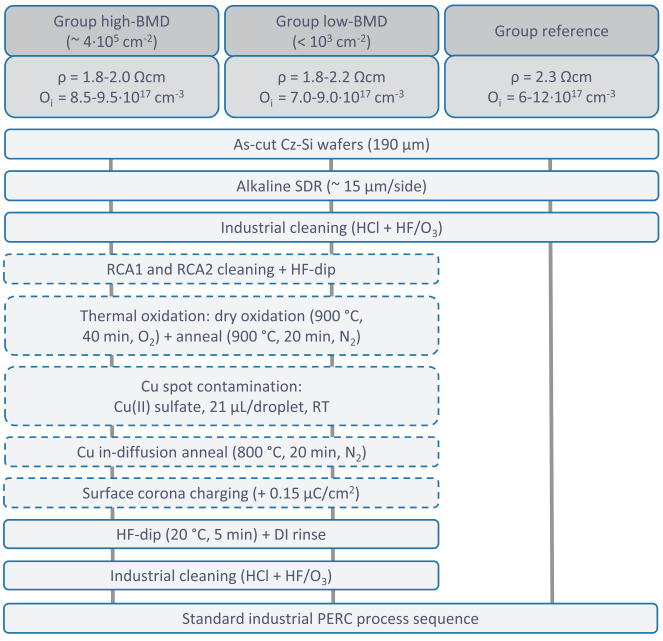

Fig. 1. Process flow chart. The PERC cells were fabricated at an industrial pilot line (solid boxes), while the Cu contamination steps were carried out using a lab-scale facility (dashed boxes). The wafers were shipped between the two different processing locations in dark boxes.

Table 1
Cu concentration in the droplets and on the wafer surface (calculated from the droplet volume and concentration).

Cu spot	[Cu] in droplet [cm^{-3}]	$[Cu]_{surface}$ [cm^{-2}]
low-Cu	$4 \cdot 10^{12}$	$1.4 \cdot 10^{12}$
mid-Cu	$6 \cdot 10^{13}$	$1.8 \cdot 10^{13}$
high-Cu	$3 \cdot 10^{14}$	$9.0 \cdot 10^{13}$

different concentration of Cu(II) sulfate solution were placed on three well-defined locations on the wafer surfaces. The droplets were poured on the side of the wafer that would later be processed into the front side of the PERC cell. To achieve homogeneous Cu concentration along the wafer thickness, drive-in of Cu species from the surface to the wafer bulk was then performed during an anneal at 800 °C for 20 min in N_2 atmosphere. It is noteworthy that the total area contaminated with the droplets corresponded to < 15% of the total wafer surface. The total concentration of Cu in each of the droplets and the corresponding surface concentration, $[Cu]_{surface}$, are reported in Table 1. $[Cu]_{surface}$ is the total Cu concentration on the wafer surface calculated from the volume and concentration of the solution droplet. The concentrations in the Cu solution were targeted to match typical Cu surface contamination present after brass wire sawing and saw damage removal etch [11] in an industrial environment [13]. After the Cu drive-in annealing, a positive corona charge (+ 0.15 μC/cm^2) was deposited on both wafer surfaces to prevent Cu out-diffusion during transportation, *i.e.* dissolved Cu_i^+ impurities would remain in the bulk due to the Coulomb field interaction with the positive corona charge on the surface, as described in Ref. [20]. Note that the use of the droplet contamination procedure allows the simultaneous presence of both Cu contaminated areas and Cu-free reference areas on the same wafer.

As the Cu-contaminated wafers arrived at SolarWorld Industries GmbH, the first step consisted in the removal of the thermal oxide layer required for the Cu spot contamination. Following this step, the wafers were then cleaned again and successively processed into PERC solar cells in their pilot line, following industrial standard processing sequence and parameters for PERC cells fabrication. Additionally, a reference group was included in the cell processing that was known to suffer only from BO-LID [21]. The as-processed efficiency and open circuit voltage, V_{oc} were 20.86% and 668 mV, respectively. All cells were processed in the same batch to limit any process-related variability. The finished cells were then degraded on-site under 0.5 suns and at 75 °C for a total of ~ 160 h.

Photoluminescence (PL) maps were collected on finished cells before and after degradation (6 h) to enable spatially-resolved imaging of the LID process, *i.e.* pixel-by-pixel subtraction of the maps in order to visualize the impact of Cu-LID in the contaminated areas. The PL maps are presented both in the undegraded stage and as ΔPL_{rel}, *i.e.* the difference between the undegraded PL intensity and the PL intensity after 6 h of degradation, normalized over the undegraded PL intensity. In addition, the evolution of the solar cell parameters were sequentially monitored during the whole degradation time on full cells (*i.e.,* measured over the whole cell area), at SolarWorld Industries characterization lab. Internal quantum efficiency (IQE) was measured at the end of degradation on one of the high-BMD group cells (over selected cell areas and at different wavelengths).

3. Results and discussion

3.1. Local degradation of PERC cells due to intentional Cu contamination

Fig. 2a shows a typical PL map taken from a finished cell from the high-BMD group before light soaking. The Cu-contaminated areas are highlighted in the PL maps by the dashed lines, serving as visual reference. As the figure shows, no clear sign of recombination caused by

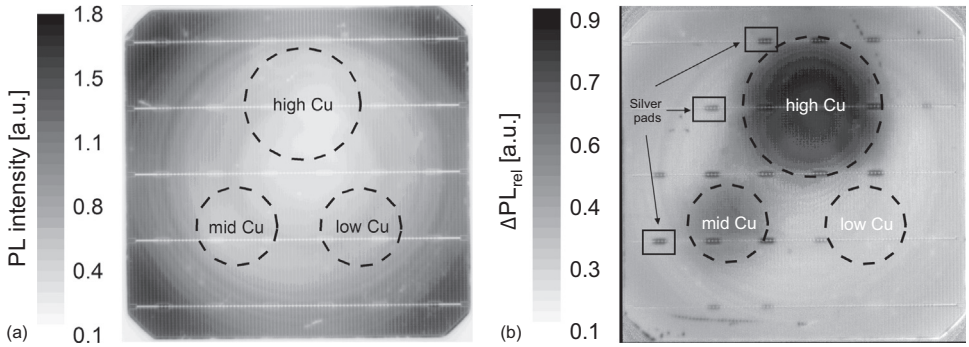

Fig. 2. (a) Undegraded PL map of a complete PERC cell from the high-BMD group. (b) PL imaging after LID on the same cell. The map shows ΔPL_{rel}, *i.e.* the normalized difference of PL maps before and after 6 h of degradation (0.5 suns, 75 °C). The dashed circles highlight the Cu contaminated areas and the black arrows point to the Ag soldering pads.

the added Cu species is visible from these undegraded cells in the contaminated areas.

Fig. 2b presents the impact of light soaking on the same cell shown in Fig. 2a, in the form of the ΔPL_{rel} map, where the dark end of the spectrum indicates areas with strong lifetime degradation during light soaking, and the light end indicates areas where no degradation occurs. The map shows that light soaking leads to various degradation strengths in the cell, *i.e.* $\Delta PLrel > 0$ over the whole cell area. While the modest background degradation was likely due to BO-LID, two highly degraded areas clearly appeared in correspondence of the locations where the mid-Cu and high-Cu droplets were originally deposited (Fig. 2b). Note that the degradation is the strongest on the high-Cu area, whereas it is below the PL detection limit for the low-Cu area. These results provide clear evidence that Cu-LID occurs in the final cells and that PERC cell fabrication does not necessarily getter Cu from the wafer bulk. This is consistent with recent experimental results obtained with lifetime samples [22].

Additionally, it is interesting to notice from the ΔPL_{rel} maps that the rear-side silver soldering pads (indicated by the black arrows in Fig. 2b) show a much stronger degradation compared to the neighbouring areas for both the mid-Cu and high-Cu areas. Since there is no Al-BSF under the soldering pads, the degradation under the soldering pads is likely to arise from the absence of Al-gettering in those locations. This is in contrast to Al-BSF that is present under local point contacts that are densely distributed on the backside of the wafer. This result leads us to speculate that Cu-LID would not be so severe in Al-BSF cells due to effective Al-gettering, contrarily to PERC cells.

To map the impact of Cu-LID on local cell performance, the IQE spectra were measured after degradation for ~ 160 h on several cell areas with varying Cu concentrations (Fig. 3). The impact of Cu contamination on IQE is distinct, and it has a direct correlation with the Cu concentration. In addition, the IQE spectra readily confirm that the Cu-LID is caused by bulk or back surface recombination, as the IQE

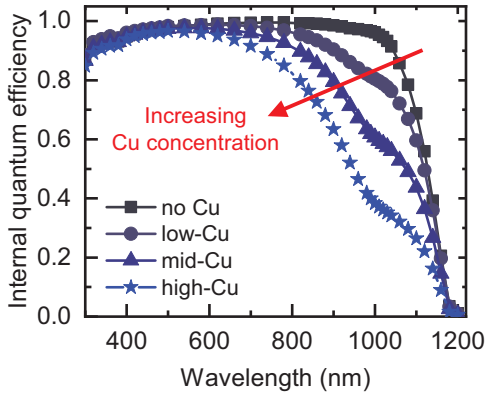

Fig. 3. IQE spectra measured on selected areas within the differently contaminated areas on a cell from the high-BMD group after 6 h of light soaking. The reference area is measured on the bottom right in the map in Fig. 2a.

decrease is mainly seen in wavelengths above 800 nm. It was then confirmed by calculations [23] that the decrease in IQE is indeed a bulk effect as the resulting bulk diffusion lengths in the high-Cu area and in the reference (non-Cu-contaminated) area were found to be 56 µm and > 700 µm, respectively.

Interestingly, the IQE is greatly affected even with the lowest Cu concentration, albeit it was not visible in the PL maps taken after 6 h of degradation (Fig. 2b). The corresponding decreases in the short circuit current density, j_{sc}, compared to the reference area (40.0 mA/cm^2) measured at the same degradation time are reported in Table 2. These numbers show that in case the full cell area were to be contaminated with the same copper concentration, *e.g.* 2×10^{13} cm^{-2} (mid-Cu spot), the impact of j_{sc} only on the final cell efficiency would be at least 10%. However, it is likely that also the V_{oc} would be greatly reduced due to increased bulk recombination, thus affecting the final cell efficiency even more.

3.2. Impact of intentional Cu contamination spots on total PERC cell efficiency

The IQE data above provided some idea of the impact of Cu-LID on the full cell parameters. However, in our experiments the total Cu contaminated area was only < 15% of the total cell area, thus making direct correlation of the surface contamination level with the cell parameters challenging. Nevertheless, the local degradation is still strong enough to leave a fingerprint on the parameters of the entire cell. This is seen in the decrease of the full solar cell parameters reported in Table 3, measured after 23 h of light soaking. The degradation of the cell efficiency corresponds to a relative degradation of 6.6% compared to the initial value (*i.e.* measured before light soaking). As mentioned above, since only specific cell areas were Cu contaminated, it is reasonable to expect much stronger degradation if the entire cell had been homogenously contaminated.

3.3. Impact of the crystal quality of the silicon substrate on the Cu-LID

The results presented above considered only the high-BMD wafers, whereas in the following we include the low-BMD group to study the impact of the crystal quality. Both groups showed no sign of the impact of the Cu-contaminated areas before light soaking (see Fig. 2a and Fig. 4a for the high-BMD and the low-BMD groups, respectively). However, after light soaking the two groups showed quite different

Table 2
Short circuit current density, j_{sc} decrease in the Cu-contaminated spots: percentage decrease compared to the non-Cu-contaminated area (reference, with j_{sc} of 40 mA/cm^2) in a cell from the high-BMD group.

Integrated spectrum (wavelength)	Low-Cu	Mid-Cu	High-Cu
300–1200 nm	4%	11%	19%
900–1200 nm	14%	34%	56%

Table 3
Normalized values of the full cell parameters for high-BMD cells after full degradation. Normalization over the undegraded value and light soaking occurring under 0.5 suns and at 75 °C. Maximum degradation at ~ 23 h for all parameters, except for FF (for which it occurs at ~ 160 h).

Group	η_{min}/η_0 ($\%_{rel}$)	$V_{OC,min}/V_{OC,0}$ ($\%_{rel}$)	$J_{SC,min}/J_{SC,0}$ ($\%_{rel}$)	FF_{min}/FF_0 ($\%_{rel}$)
High-BMD	93.4	98.7	96.0	98.1

degradation behaviour, as can be seen comparing Fig. 2b (high-BMD) and Fig. 4b (low-BMD). While clear Cu-LID is seen in the cells of the high-BMD group, those of the low-BMD group did not show Cu-related degradation observable in the PL maps. Since the primary difference between the two groups of silicon substrates is the BMD density, these results point to a dependence of the extent of Cu-LID on the substrate crystal quality and thus likely on the density of oxygen precipitates or other crystal defects such as vacancy clusters or dislocation in the bulk of the wafers. Hence, it is possible that also the gettering efficiency depends on the BMD density and thus in high-BMD samples Cu is trapped in the bulk by oxygen related defects and cannot be efficiently gettered to the emitter. An alternative explanation could be that the gettering efficiency is the same in both groups but due to the lack of nucleation sites in the bulk in the low-BMD cells, Cu remains interstitial during light soaking.

The behaviour of the low-BMD group is further confirmed by the cell parameters observed during degradation. Fig. 5 reports the degradation of the cell efficiency (measured on the full cells) for both the low-BMD and high-BMD groups, and it can be seen that the extent of the degradation is more than twofold for the high-BMD group. Furthermore, the low-BMD cells show degradation kinetics more usual to what observed in a control group of PERC cells processed together with the high-BMD and low-BMD cells, and which are known to have only boron-oxygen LID (reported as the BO-group in Fig. 5). The comparison of the cell parameters for the high-BMD and low-BMD groups show that the weaker degradation in the low-BMD cells is mostly due to a lower decrease of the short circuit current, as the maximum j_{sc} degradation is 0.6% and 4% (normalized over the undegraded values) for the low-BMD and high-BMD groups, respectively. The corresponding degraded values for V_{oc} are 99.2% and 98.6% for the low-BMD and high-BMD groups, respectively.

As seen from Fig. 5, the full cells showed also clear efficiency regeneration after the 23 h of light soaking. While the BO-LID control group shows complete regeneration, Cu-contaminated cells (both high-BMD and low-BMD groups) show only partial regeneration. Notice that the Cu-LID component in the low-BMD group is below the detection limit of the PL technique. The partial regeneration has been shown earlier to be characteristic for Cu-LID and speculated to be related to dissolution of small Cu precipitates [9]; however, the exact mechanism is still under investigation.

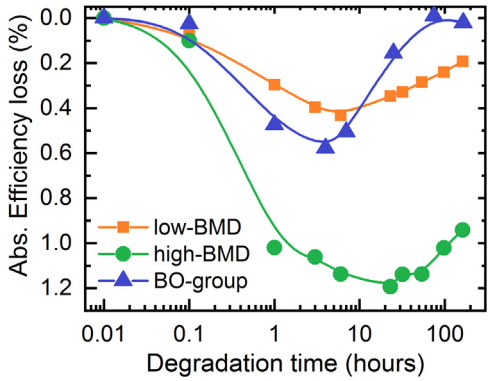

Fig. 5. Absolute cell efficiency variation (average of 3 and 2 cells for the high-BMD and the low-BMD groups, respectively) of the full cells under degradation (0.5 suns, 75 °C). A control group, known to have only BO-LID and subjected to the same cell processing parameters (as-processed efficiency and open circuit voltage, V_{oc} were 20.86% and 668 mV, respectively), is shown for comparison. The solid lines serve as guidelines for the eyes.

4. Conclusion

In this study, we demonstrate for the first time the persistence of relevant Cu concentrations in the wafer bulk after processing of industrial p-type Cz-PERC cells, which result in significant Cu-LID in the final cells. Although only specific substrate areas were intentionally contaminated (< 15% of the total cell area), we measure total cell efficiency degradation up to 6.6% relative, accompanied by a severe reduction of internal quantum efficiency and short circuit current density (up to 19% lower in high-Cu concentration areas compared to the reference areas).

We also find a correlation between the strength of cell efficiency degradation and the substrate crystal quality, *i.e.* stronger degradation is measured in cells manufactured from substrates with higher etch pit density. Hence, we conclude that the substrate quality is an important parameter, which not only affects the relevance of degradation effects but gives also insights on the tolerable Cu concentration for high-efficiency solar cell manufacture.

This work also reports indications that the gettering efficiency of PERC cells may be lower compared to Al-BSF cells, which would make the PERC cells more sensitive to metal contamination.

Acknowledgements

The work was partially funded through the European Research Council under the European Union's FP7 Programme ERC Grant Agreement No. 307315. Dr. Moises Garin (Polytechnic University of Catalonia) is kindly acknowledged for the short circuit current calculations. H. S. L. acknowledges the support of Tiina and Antti Herlin

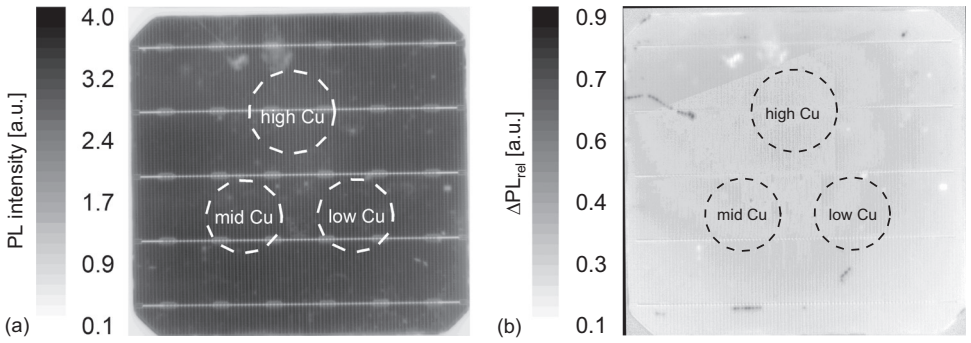

Fig. 4. (a) Undegraded PL map of a full PERC cell from the low-BMD group. (b) PL imaging after LID on the same cell. The map shows ΔPL_{rel}, *i.e.* the normalized difference of PL maps before and after 6 h of degradation (0.5 suns, 75 °C). The circles highlight the Cu contaminated areas.

Foundation and the Finnish Cultural Foundation.

References

[1] International Technology Roadmap for Photovoltaic (ITRPV) incl. maturity report. ⟨http://www.itrpv.net/Reports/Downloads/⟩.

[2] F. Fertig, R. Lantzsch, A. Mohr, M. Schaper, M. Bartzsch, D. Wissen, F. Kersten, A. Mette, S. Peters, A. Eidner, J. Cieslak, K. Duncker, M. Junghänel, E. Jarzembowski, M. Kauert, B. Faulwetter-Quandt, D. Meißner, B. Reiche, S. Geißler, S. Hörnlein, C. Klenke, L. Niebergall, A. Schönmann, A. Weihrauch, F. Stenzel, A. Hofmann, T. Rudolph, A. Schwabedissen, M. Gundermann, M. Fischer, J.W. Müller, D.J.W. Jeong, Mass production of p-type Cz silicon solar cells approaching average stable conversion efficiencies of 22%, Energy Procedia 124 (2017) 338–345, https://doi.org/10.1016/j.egypro.2017.09.308.

[3] F. Kersten, F. Fertig, K. Petter, B. Klöter, E. Herzog, M.B. Strobel, J. Heitmann, J.W. Müller, System performance loss due to LeTID, Energy Procedia 124 (2017) 540–546, https://doi.org/10.1016/j.egypro.2017.09.260.

[4] B. Hallam, A. Herguth, P. Hamer, N. Nampalli, S. Wilking, M. Abbott, S. Wenham, G. Hahn, Eliminating light-induced degradation in commercial p-Type Czochralski silicon solar cells, Appl. Sci. 8 (2018), https://doi.org/10.3390/app8010010.

[5] F. Wolny, T. Weber, M. Müller, G. Fischer, Light induced degradation and regeneration of high efficiency Cz PERC cells with varying base resistivity, Energy Procedia 38 (2013) 523–530, https://doi.org/10.1016/j.egypro.2013.07.312.

[6] M. Xie, C. Ren, L. Fu, X. Qiu, D. Yang, An industrial solution to light-induced degradation of crystal- line silicon solar cells, Front. Energy 11 (2017) 67–71, https://doi.org/10.1007/s11708-016-0430-x.

[7] J. Lindroos, H. Savin, Review of light-induced degradation in crystalline silicon solar cells, Sol. Energy Mater. Sol. Cells 147 (2016) 115–126, https://doi.org/10.1016/j.solmat.2015.11.047.

[8] H. Vahlman, A. Haarahiltunen, W. Kwapil, J. Schön, A. Inglese, H. Savin, Modeling of light-induced degradation due to Cu precipitation in p-type silicon. I. General theory of precipitation under carrier injection, J. Appl. Phys. 121 (2017) 195703, https://doi.org/10.1063/1.4983454.

[9] H. Vahlman, A. Haarahiltunen, W. Kwapil, J. Schön, A. Inglese, H. Savin, A. Haarahiltunen, W. Kwapil, J. Schön, A. Inglese, H. Savin, Modeling of light-induced degradation due to Cu precipitation in p-type silicon. II. Comparison of simulations and experiments, J. Appl. Phys. 121 (2017) 195704, https://doi.org/10.1063/1.4983455.

[10] J. Hofstetter, J.F. Lelièvre, C. del Cañizo, A. Luque, Acceptable contamination levels in solar grade silicon: from feedstock to solar cell, Mater. Sci. Eng. B 159–160 (2009) 299–304, https://doi.org/10.1016/j.mseb.2008.05.021.

[11] F. Buchholz, E. Wefringhaus, G. Schubert, Metal surface contamination during phosphorus diffusion, Energy Procedia 27 (2012) 287–292, https://doi.org/10.1016/j.egypro.2012.07.065.

[12] A.A. Istratov, E.R. Weber, Physics of Copper in Silicon, J. Electrochem. Soc. 149 (2002) G21–G30, https://doi.org/10.1149/1.1421348.

[13] H. Vahlman, M. Wagner, F. Wolny, A. Krause, H. Laine, A. Inglese, M. Yli-koski, H. Savin, Light-induced degradation in quasi-monocrystalline silicon PERC solar cells: indications on involvement of copper, Phys. Status Solidi 214 (2017) 1700321, https://doi.org/10.1002/pssa.201700321.

[14] T. Turmagambetov, S. Dubois, J.P. Garandet, B. Martel, N. Enjalbert, J. Veirman, E. Pihan, Influence of copper contamination on the illuminated forward and dark reverse current-voltage characteristics of multicrystalline p-type silicon solar cells, Phys. Status Solidi Curr. Top. Solid State Phys. 11 (2014) 1697–1702, https://doi.org/10.1002/pssc.201400036.

[15] K. Bothe, J. Schmidt, Fast-forming boron-oxygen-related recombination center in crystalline, Appl. Phys. Lett. 87 (2005) 262108, https://doi.org/10.1063/1.2147727.

[16] P. Saint-Cast, I. Reis, J. Greulich, S. Werner, E. Lohmüller, H. Höffler, J. Haunschild, R. Preu, Cz silicon benchmark for p-type PERC solar cells, in: Proceedings of the 32nd EUPVSEC: 2016: pp. 1038–1043.

[17] H. Väinölä, E. Saarnilehto, M. Yli-Koski, A. Haarahiltunen, J. Sinkkonen, G. Berenyi, T. Pavelka, Quantitative copper measurement in oxidized p-type silicon wafers using microwave photoconductivity decay, Appl. Phys. Lett. 87 (2005) 032109, https://doi.org/10.1063/1.1999008.

[18] F. Wolny, A. Krause, A. Oehlke, M. Wagner, Wafer FTIR - measuring interstitial oxygen on as cut and processed silicon wafers, Energy Procedia 92 (2016) 274–277, https://doi.org/10.1016/j.egypro.2016.07.076.

[19] H. Savin, M. Yli-koski, A. Haarahiltunen, Role of copper in light induced minority-carrier lifetime degradation of silicon, Appl. Phys. Lett. 95 (2009) 152111, https://doi.org/10.1063/1.3250161.

[20] Y. Boulfrad, J. Lindroos, M. Wagner, F. Wolny, M. Yli-Koski, H. Savin, Experimental evidence on removing copper and light-induced degradation from silicon by negative charge, Appl. Phys. Lett. 105 (2014) 2014–2017, https://doi.org/10.1063/1.4901533.

[21] T.U. Nærland, H. Haug, H. Angelskår, R. Søndenå, E.S. Marstein, L. Arnberg, Studying light-induced degradation by lifetime decay analysis: excellent fit to solution of simple second-order rate equation, IEEE J. Photovolt. 3 (2013) 1265–1270.

[22] A. Inglese, H.S. Laine, V. Vähänissi, H. Savin, Cu gettering by phosphorus-doped emitters in p -type silicon: effect on light-induced degradation, AIP Adv. 8 (2018) 015112.

[23] D.K. Schroder, Surface voltage and surface photovoltage: history, theory and applications, Meas. Sci. Technol. 12 (2001) R16–R31, https://doi.org/10.1088/0957-0233/12/3/202.